LETTER

https://doi.org/10.1038/s41586-018-0468-5

A complex dynamo inferred from the hemispheric dichotomy of Jupiter's magnetic field

Kimberly M. Moore[1], Rakesh K. Yadav[1], Laura Kulowski[1], Hao Cao[1], Jeremy Bloxham[1]*, John E. P. Connerney[2,3], Stavros Kotsiaros[2,4], John L. Jørgensen[5], José M. G. Merayo[5], David J. Stevenson[6], Scott J. Bolton[7] & Steven M. Levin[8]

The Juno spacecraft, which is in a polar orbit around Jupiter, is providing direct measurements of the planet's magnetic field close to its surface[1]. A recent analysis of observations of Jupiter's magnetic field from eight (of the first nine) Juno orbits has provided a spherical-harmonic reference model (JRM09)[2] of Jupiter's magnetic field outside the planet. This model is of particular interest for understanding processes in Jupiter's magnetosphere, but to study the field within the planet and thus the dynamo mechanism that is responsible for generating Jupiter's main magnetic field, alternative models are preferred. Here we report maps of the magnetic field at a range of depths within Jupiter. We find that Jupiter's magnetic field is different from all other known planetary magnetic fields. Within Jupiter, most of the flux emerges from the dynamo region in a narrow band in the northern hemisphere, some of which returns through an intense, isolated flux patch near the equator. Elsewhere, the field is much weaker. The non-dipolar part of the field is confined almost entirely to the northern hemisphere, so there the field is strongly non-dipolar and in the southern hemisphere it is predominantly dipolar. We suggest that Jupiter's dynamo, unlike Earth's, does not operate in a thick, homogeneous shell, and we propose that this unexpected field morphology arises from radial variations, possibly including layering, in density or electrical conductivity, or both.

Unlike Earth, for which the top of the dynamo region is well defined by the core–mantle boundary—that is, the boundary between the electrically conducting liquid-iron outer core (in which dynamo action occurs) and the overlying, poorly conducting rocky mantle—for Jupiter the corresponding region is less clearly defined. Even though self-sustaining dynamo action is most probably confined to depths below the metallic-hydrogen transition, the field may be affected by flow in the overlying molecular-hydrogen region[3–5], which may have substantial electrical conductivity, especially close to the depth of the metallic-hydrogen transition[6,7]. Accordingly, we map the field at four equally spaced radii from the surface of Jupiter (corresponding to $r = R_J = 71{,}492$ km, where R_J is Jupiter's radius), at which the electrical conductivity is vanishingly small, to $r = 0.85R_J$, the likely depth of the metallic-hydrogen transition.

To do so requires mapping the field below the orbit of the spacecraft, and so we must address the instability due to downward continuation. We do so by regularizing the solution using a quadratic norm based on the horizontal Laplacian of the radial magnetic field, thereby finding the smoothest possible map of the field for a given fit to the observations[8]. We select Juno magnetometer observations[1] from eight orbits in the radial distance range from $r = 1.06R_J$ (perijove) to $r = 2.2R_J$ (roughly corresponding to Juno's highest latitude), take 30-s averages of the data (corresponding to one rotation of the spacecraft) and weight the data according to an estimate of their measurement uncertainty. Our resulting dataset consists of 1,991 observations of each of the three components of the magnetic field.

In Fig. 1 we show maps of the radial component of the magnetic field at a range of depths using our regularized inversion from the surface to $r = 0.85R_J$ and compare with JRM09[2]. At all depths, positive radial flux in the northern hemisphere is confined to a band (the northern-hemisphere flux band), which becomes narrower with depth. Some of the flux from this band then re-enters through an intense spot on the equator[9] (the Great Blue Spot), at a longitude of around 90° west (in System III coordinates). The morphology of the magnetic field lines is shown in Fig. 2 (an animated version of Fig. 2 is available at https://doi.org/10.6084/m9.figshare.6828953). Elsewhere, and corresponding to a large proportion of the surface, the radial flux is much weaker.

The narrowing of the northern-hemisphere flux band with depth, and more generally the concentration of flux into increasingly localized regions with depth rather than, for example, the emergence of more small-scale spots, is surprising given our intuition acquired from mapping Earth's magnetic field at depth. It suggests that Jupiter's magnetic field at depth may be morphologically simpler than expected. This field morphology and its contrast to Earth's field is particularly apparent in Fig. 3, in which we show the non-dipolar part of the field (at $r = 0.90R_J$) and, for comparison, Earth's non-dipole field (at Earth's core–mantle boundary). Jupiter's non-dipole field is almost entirely confined to the northern hemisphere, where the non-dipole field peaks at 3 mT, a value almost three times stronger than the peak dipolar field. Jupiter's field is dipolar in the southern hemisphere and largely non-dipolar in the northern hemisphere, unlike Earth's field.

The strong concentration of magnetic flux in the northern-hemisphere flux band and in the Great Blue Spot implies the existence of large horizontal magnetic field gradients at the borders of these features, which would suggest that strong secular (temporal) variation of the magnetic field is likely. For example, around the Great Blue Spot the gradient in the radial field is approximately 3 mT/(10^6 m); with an assumed flow speed of the order of 10^{-4} m s^{-1} (the lower end of estimates of flow speed[10,11]), we might therefore expect secular variation of the order of 10^4 nT yr^{-1}. Although high, this estimate is not necessarily inconsistent with earlier inferences of much weaker time dependency[12] because secular variation at such small spatial scales would be strongly attenuated at the altitude of the previous observations. In addition, this estimate will be reduced if the flow is preferentially orthogonal to the field gradient, although for the Great Blue Spot that is unlikely on geometrical grounds to be the case. Therefore, we believe that the Great Blue Spot offers a very promising opportunity for forthcoming Juno orbits to detect secular variation.

Numerical dynamo models in simple homogeneous shells typically produce fields that are either strongly dipolar or dominated by multipolar fields[10,13]. Jupiter's field is neither, being predominantly dipolar in one hemisphere and non-dipolar in the other, suggesting that the field is not generated in a simple homogeneous region. Here we consider several possible explanations. First, we consider the possibility, although unlikely, that we have observed the field in a rare transitional

[1]Department of Earth and Planetary Sciences, Harvard University, Cambridge, MA, USA. [2]NASA/GSFC, Greenbelt, MD, USA. [3]Space Research Corporation, Annapolis, MD, USA. [4]University of Maryland, College Park, MD, USA. [5]National Space Institute, Technical University of Denmark, Kongens Lyngby, Denmark. [6]Division of Geological and Planetary Sciences, California Institute of Technology, Pasadena, CA, USA. [7]Southwest Research Institute, San Antonio, TX, USA. [8]Jet Propulsion Laboratory, California Institute of Technology, Pasadena, CA, USA.
*e-mail: jeremy_bloxham@harvard.edu

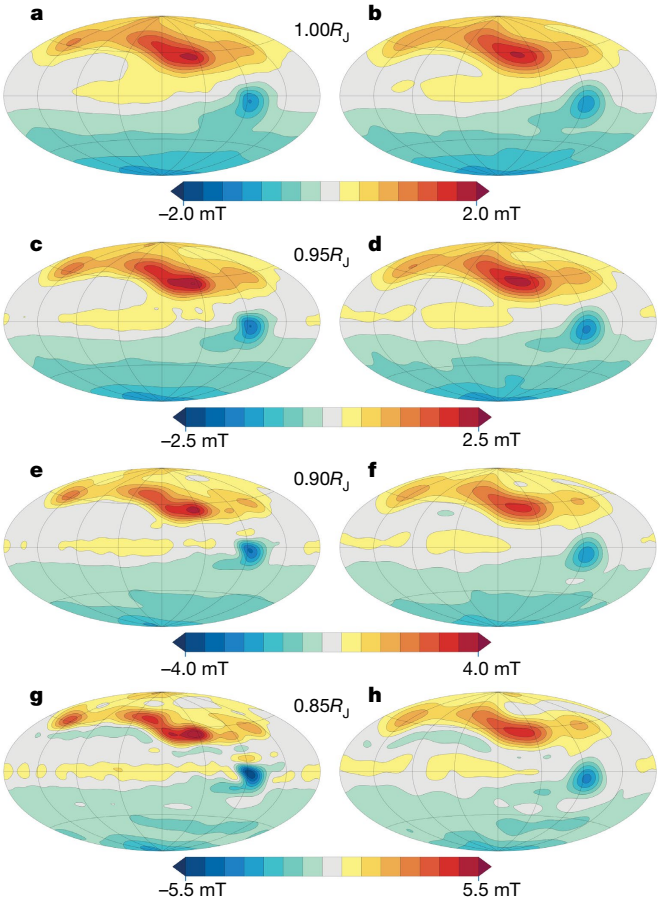

Fig. 1 | The radial component of Jupiter's magnetic field. The plots are shown on a Hammer equal-area projection with the central meridian at a longitude of 180° west (System III coordinates). The colour scale depicts the strength of the radial component of the magnetic field, with yellow–red shades depicting field in the positive radial direction (outwards) and green–blue shades depicting field in the negative radial direction (inwards). **a**, **b**, A regularized solution (**a**) and the JRM09 solution (**b**) at $r = 1.00R_J$; **c**, **d**, the same at $r = 0.95R_J$; **e**, **f**, the same at $r = 0.90R_J$; **f**, **g**, the same at $r = 0.85R_J$. Although the regularized solution and the JRM09 solution have a similar pattern at each depth, the regularized solution reveals more intense and concentrated field structure. Overall, the same basic field morphology is apparent across the range of depths and the two models.

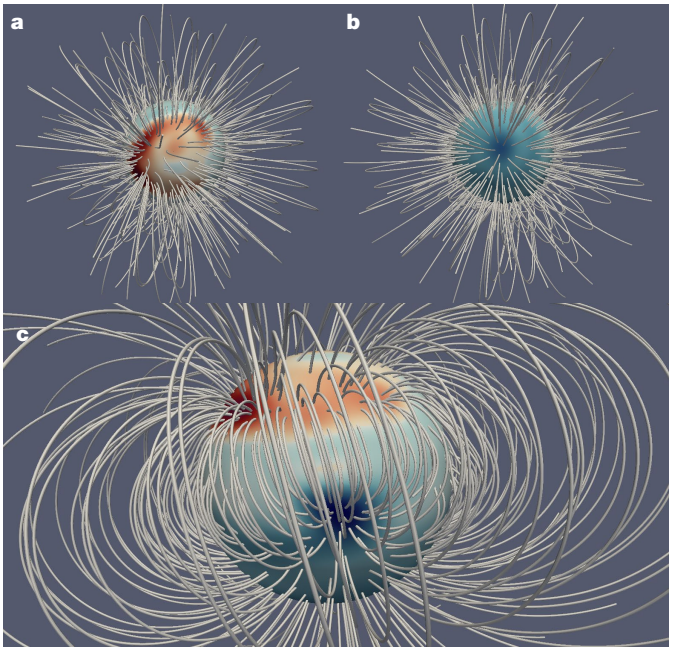

Fig. 2 | Magnetic field lines. a, North polar view; **b**, south polar view; **c**, equatorial view. The non-dipolar nature of the magnetic field in the northern hemisphere and the dipolar nature in the southern hemisphere is apparent. The equatorial view is centred near the Great Blue Spot and shows the linkage of magnetic field lines that enter through the Great Blue Spot. The contoured surface on which the field lines shown start and end is at $r = 0.85R_J$, where the density of field lines is proportional to the radial magnetic field strength and is depicted by the colour scale (red outward flux, blue inward flux). An animated version of this figure is available at https://doi.org/10.6084/m9.figshare.6828953.

state, such as a magnetic field reversal or a transition between different dynamo states[14,15]. However, such a situation cannot necessarily be reconciled with the co-existence of strong dipole and non-dipole fields. Instead, we next consider whether Jupiter's internal structure could account for the observations.

Starting near the top of Jupiter's dynamo region, there is the possibility of a stably stratified layer due to precipitation of helium[16]. Such a layer might axisymmetrize the field[17], but could also destabilize the field[18]. However, this scenario also seems unlikely to be able to account for the observed hemispheric difference in the field morphology. There is also the effect of the steep gradient in electrical conductivity immediately above the metallic-hydrogen transition[7]. A recent numerically simulated dynamo including this effect shows irregular behaviour[19], with one snapshot appearing similar to the Juno-determined field. This is a possibility that requires further investigation. Finally, another recent study[20] has examined flow and the generation of magnetic fields in Jupiter for three scenarios that involve near-surface layering, although none of the scenarios produces magnetic fields similar to that observed by Juno.

At depth, other processes may be important. In particular, the mixture of rock and ice that probably constitutes (or constituted) Jupiter's core will be soluble in hydrogen at the temperature and pressure expected there[21–25]. This may lead to gradual core dissolution, and may have been crucial in Jupiter's thermal history[26,27]. Dissolution of rock and ice in metallic hydrogen will increase the density of the hydrogen region. Recent Juno observations of Jupiter's gravity field are consistent with the existence of a partially or fully dissolved core inside Jupiter, with rock and ice non-uniformly mixed in the hydrogen out to approximately half the radius of the planet[28]; the region further out may be homogeneous, except for helium rain.

If, as theory and observations suggest, the metallic-hydrogen region is layered (the upper layer solute-free and the lower layer containing dissolved rock and ice), the implications for the dynamo will depend on the convective instability of these layers. The upper layer is most probably convectively unstable, given the very large heat flux observed at Jupiter. The properties of the lower layer are far less clear. If the lower layer is stable, then dynamo action will be confined to the upper layer and will therefore operate in a shell with a radius ratio (inner to outer radii) of approximately 0.5. A similar geometry has been investigated previously as a possible explanation for the magnetic fields of Uranus and Neptune[29], albeit with a numerical dynamo model much less sophisticated than what is now feasible. The magnetic field map obtained from this simulation with a radius ratio of 0.5 (see figure 16, model 5 in ref. 29) bears similarity to the map of Jupiter's field shown here, but with an axial dipole that is much less dominant. In addition, structure may arise from double diffusive convection[26].

Alternatively, if the lower layer is convectively unstable, then it could be convecting separately from the layer above owing to the possible presence of a density jump at the boundary between the layers[28]. Convection in Jupiter's metallic-hydrogen region can be driven by relative density variations ($\Delta\rho/\rho$) of the order of 10^{-6}, so even a small density jump could be impervious to convection. In this scenario, dynamo action may occur separately in the thick lower shell

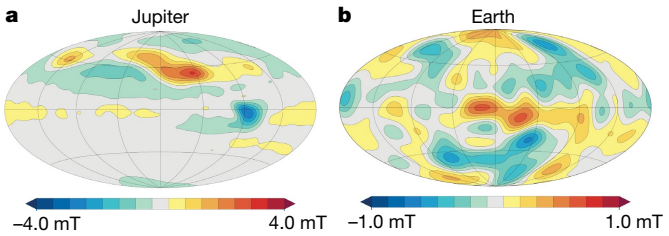

Fig. 3 | Non-dipole radial field. a, The non-dipolar part of Jupiter's radial magnetic field at $r = 0.90R_J$. **b**, For comparison, the non-dipolar part of Earth's radial magnetic field at the core–mantle boundary ($r = 0.55R_E = 3{,}485$ km, where R_E is Earth's radius). Almost all of Jupiter's non-dipole radial field is concentrated in the northern hemisphere, whereas Earth's field is evenly distributed throughout.

(radius ratio of less than 0.2) and in the thin upper shell (radius ratio of approximately 0.5), with the resultant field sharing properties of both a thick-shell dynamo (strong axial dipole) and a relatively thin-shell dynamo (hemispheric asymmetry).

The presence or absence of reduced magnetic flux at high latitude may provide a means of distinguishing between these alternatives. If the lower layer is stably stratified, then convection in the outer layer within the tangent cylinder (the axial cylinder tangential to the interface between the two layers) may differ from that outside the tangent cylinder. If the lower layer is convectively unstable, then such an effect seems less likely to occur. To resolve this additional Juno orbits are required. Juno's orbit, with perijove precessing northward by approximately 1° per orbit, is evolving in such a way that mid- and high-latitude structure will be better resolved towards the second half of the planned 34-orbit baseline mission[30].

Data availability

The Juno magnetometer data used in this study will be made available through the NASA Planetary Data System (https://pds.nasa.gov) in accordance with NASA policy. An animated version of Fig. 2 is available at https://doi.org/10.6084/m9.figshare.6828953.

Received: 9 April 2018; Accepted: 26 July 2018;
Published online 5 September 2018.

1. Connerney, J. E. P. et al. The Juno magnetic field investigation. *Space Sci. Rev.* **213**, 39–138 (2017).
2. Connerney, J. E. P. et al. A new model of Jupiter's magnetic field from Juno's first nine orbits. *Geophys. Res. Lett.* **45**, 2590–2596 (2018).
3. Liu, J., Goldreich, P. M. & Stevenson, D. J. Constraints on deep-seated zonal winds inside Jupiter and Saturn. *Icarus* **196**, 653–664 (2008).
4. Gastine, T., Wicht, J., Duarte, L., Heimpel, M. & Becker, A. Explaining Jupiter's magnetic field and equatorial jet dynamics. *Geophys. Res. Lett.* **41**, 5410–5419 (2014).
5. Cao, H. & Stevenson, D. J. Zonal flow magnetic field interaction in the semi-conducting region of giant planets. *Icarus* **296**, 59–72 (2017).
6. Nellis, W. J., Weir, S. T. & Mitchell, A. C. Metallization and electrical conductivity of hydrogen in Jupiter. *Science* **273**, 936–938 (1996).
7. French, M. et al. Ab initio simulations for material properties along the Jupiter adiabat. *Astrophys. J. Suppl. Ser.* **202**, 5 (2012).
8. Shure, L., Parker, R. L. & Backus, G. E. Harmonic splines for geomagnetic modelling. *Phys. Earth Planet. Inter.* **28**, 215–229 (1982).
9. Moore, K. M., Bloxham, J., Connerney, J. E. P., Jørgensen, J. L. & Merayo, J. M. G. The analysis of initial Juno magnetometer data using a sparse magnetic field representation. *Geophys. Res. Lett.* **44**, 4687–4693 (2017).
10. Christensen, U. R. & Aubert, J. Scaling properties of convection-driven dynamos in rotating spherical shells and application to planetary magnetic fields. *Geophys. J. Int.* **166**, 97–114 (2006).
11. Jones, C. A. A dynamo model of Jupiter's magnetic field. *Icarus* **241**, 148–159 (2014).
12. Ridley, V. A. & Holme, R. Modeling the Jovian magnetic field and its secular variation using all available magnetic field observations. *J. Geophys. Res. Planets* **121**, 309–337 (2016).
13. Jones, C. A. Planetary magnetic fields and fluid dynamos. *Annu. Rev. Fluid Mech.* **43**, 583–614 (2011).
14. Duarte, L. D. V., Wicht, J. & Gastine, T. Physical conditions for Jupiter-like dynamo models. *Icarus* **299**, 206–221 (2018).
15. Grote, E. & Busse, F. H. Hemispherical dynamos generated by convection in rotating spherical shells. *Phys. Rev. E* **62**, 4457–4460 (2000).
16. Salpeter, E. E. On convection and gravitational layering in Jupiter and in stars of low mass. *Astrophys. J.* **181**, L83–L86 (1973).
17. Stevenson, D. J. Reducing the non-axisymmetry of a planetary dynamo and an application to Saturn. *Geophys. Astrophys. Fluid Dyn.* **21**, 113–127 (1982).
18. Stanley, S. & Mohammadi, A. Effects of an outer thin stably stratified layer on planetary dynamos. *Phys. Earth Planet. Inter.* **168**, 179–190 (2008).
19. Dietrich, W. & Jones, C. A. Anelastic spherical dynamos with radially variable electrical conductivity. *Icarus* **305**, 15–32 (2018).
20. Glatzmaier, G. A. Computer simulations of Jupiter's deep internal dynamics help interpret what Juno sees. *Proc. Natl Acad. Sci. USA* **115**, 6896–6904 (2018).
21. Stevenson, D. J. Cosmochemistry and structure of the giant planets and their satellites. *Icarus* **62**, 4–15 (1985).
22. Wilson, H. F. & Militzer, B. Rocky core solubility in Jupiter and giant exoplanets. *Phys. Rev. Lett.* **108**, 111101 (2012).
23. Wilson, H. F. & Militzer, B. Solubility of water ice in metallic hydrogen: consequences for core erosion in gas giant planets. *Astrophys. J.* **745**, 54 (2012).
24. Wahl, S. M., Wilson, H. F. & Militzer, B. Solubility of iron in metallic hydrogen and stability of dense cores in giant planets. *Astrophys. J.* **773**, 95 (2013).
25. González-Cataldo, F., Wilson, H. F. & Militzer, B. Ab initio free energy calculations of the solubility of silica in metallic hydrogen and application to giant planet cores. *Astrophys. J.* **787**, 79 (2014).
26. Helled, R. & Stevenson, D. The fuzziness of giant planets' cores. *Astrophys. J. Lett.* **840**, L4 (2017).
27. Vazan, A., Helled, R. & Guillot, T. Jupiter's evolution with primordial composition gradients. *Astron. Astrophys.* **610**, L14 (2018).
28. Wahl, S. M. et al. Comparing Jupiter interior structure models to Juno gravity measurements and the role of a dilute core. *Geophys. Res. Lett.* **44**, 4649–4659 (2017).
29. Stanley, S. & Bloxham, J. Numerical dynamo models of Uranus' and Neptune's magnetic fields. *Icarus* **184**, 556–572 (2006).
30. Bolton, S. J. et al. The Juno mission. *Space Sci. Rev.* **213**, 5–37 (2017).

Acknowledgements All authors acknowledge support from the Juno project. K.M.M. is supported by the US Department of Defense (DoD) through the National Defense Science and Engineering Graduate Fellowship (NDSEG) programme and L.K. through a US National Science Foundation Graduate Fellowship.

Reviewer information *Nature* thanks C. Jones and the other anonymous reviewer(s) for their contribution to the peer review of this work.

Author contributions K.M.M. and J.B. wrote the manuscript and performed the data analysis. K.M.M., J.B., J.E.P.C., S.K., J.L.J. and J.M.G.M. contributed to discussions of the data analysis, and K.M.M., R.K.Y., L.K., H.C., J.B. and D.J.S. contributed to discussions of the dynamo implications. All authors contributed to editing and revising the manuscript. J.E.P.C. is principal investigator of the Juno magnetometer investigation, S.J.B. is principal investigator of the mission and S.M.L. is project scientist of the mission.

Competing interests The authors declare no competing interests.

Additional information
Reprints and permissions information is available at http://www.nature.com/reprints.
Correspondence and requests for materials should be addressed to J.B.
Publisher's note: Springer Nature remains neutral with regard to jurisdictional claims in published maps and institutional affiliations.